Quaternary International 374 (2015) 182–188

Contents lists available at ScienceDirect

Quaternary International

journal homepage: www.elsevier.com/locate/quaint

Forum communication

A large and active debris-rockslide in the Central Andes of Argentina (30.26°S): Morphometry and triggering mechanisms

María Yanina Esper Angillieri*, Laura P. Perucca

CONICET – Gabinete de Neotectónica y Geomorfología, INGEO, Facultad de Ciencias Exactas, Físicas y Naturales, Universidad Nacional de San Juan, Av. José I. de la Roza y Meglioli, Rivadavia, San Juan 5400, Argentina

ARTICLE INFO

Article history:
Available online 29 December 2014

Keywords:
Debris-rockslide
Morphometry
Triggering mechanisms
GIS
Argentina

ABSTRACT

A large (>0.1 km^2) and complex mass movement in the Central Andes of Argentina (final portion of Cordillera de Olivares, Frontal Cordillera), was studied to identify the triggering factors and understand their relationship with geomorphic, cryogenic and climatic dynamics. This debris-rockslide is composed of clast supported blocks of Permian–Triassic volcanic breccias. In order to characterize this feature, high resolution satellite imagery interpretation was carried out, together with the study of the landslide detachment zones and landslide bodies. These debris-rockslide events could have originated as a consequence of the combination of internal slow deformation and fragmentation under periglacial conditions, followed by a sudden collapse of the rock mass. Pre- and post-slide digital elevation models (DEMs) were created from topographical data with the help of a Geographic Information System (GIS) tool. Approximately 14.89 M m^3 of rock and debris travelled nearly 2 km from an elevation of 5023 m –4325 m asl. Although usually the origin of such catastrophic movements is related to seismically active areas with earthquakes whose magnitude frequently exceed Ms 6, our hypothesis is that this debris-rockslide event has a climatic origin caused by large snow accumulations during winters and subsequent fast meltdown processes during spring, which would have facilitated the sliding. The paper outlines the important role that snowmelt can play in the genesis and evolution of rock displacements and the importance of meteorological data, seismic catalogues, historical aerial photography and satellite images in geomorphological back-analysis.

1. Introduction

The Andes Mountain Range bordering Argentina's western boundary is affected by various natural geologic processes. Amongst these, landslides are known to occur frequently. On the southern side of Cordillera de Olivares in particular, there are numerous landslide deposits. This mountainous area is characterized by steep slopes carved by late Pleistocene glacier retreat, sparse vegetation, and intense cryoclastism. Slope failures, such as debris flows, debris falls, rock slides and rock glaciers, take place in certain areas above the glaciofluvial terraces that built up after the retreating ice (LGM). Research in other glaciated mountain ranges of the world; have emphasized the analysis of the relationship between glacier retreat and slope instability in mountain areas (Ballantyne, 2002).

A slide is a downslope movement of soil, debris or a rock mass occurring on rupture surfaces or on relatively thin zones of intense shear strain. A rock slide is the translational movement of rock which occurs along a more or less planar or gently undulating surface (Varnes, 1978). Rock slides in stronger rock formations, usually with a high degree of structural control, are extremely rapid due to a sudden loss of cohesion. Of these, rock collapses are especially fast, and involve failure of otherwise strong rock controlled by a combination of nonsystematic joints and intact rock bridges. Stronger rocks must fail by shearing along discontinuities with only isolated bridges of intact rock providing a brittle cohesive component. If there is no systematic structural pattern, we may refer to a "rock collapse" (Hungr and Evans, 2004). The rupture surface often forms an irregular, multi-faceted scar, composed of individual joint planes separated by rough zones of crushing, tensile or shear rock failure. Such sliding movement is invariably sudden and catastrophic. Rock collapses occur along steep slopes and tend to be smaller in volume than translational slides. Rock collapse is characteristic of strong, poorly structured rocks such as

* Corresponding author.
E-mail address: yaninaesper@gmail.com (M.Y. Esper Angillieri).

http://dx.doi.org/10.1016/j.quaint.2014.12.019
1040-6182/

intrusives, volcanic or of strong structured rocks whose structure is adverse to either sliding or toppling, but where sufficient jointing exists. Deformation of a weak foundation underlying the brittle strata may serve as a trigger. The movement rate is always extremely rapid. The volumes of rock collapse failures are generally limited (Hungr and Evans, 2004).

The purpose of this paper is to describe and characterize the existing active rock slide in the Cordillera de Olivares, semi-arid Andes of Argentina, aiming at identifying possible triggering mechanisms and interpret their relation to the geomorphological dynamics and cryogenic climate.

2. Study area

The Cordillera de Olivares, part of the Frontal Cordillera, is located in the Iglesia Department, 235 km from San Juan City, San Juan Province, central-west Argentina (Fig. 1). The area (31°16′S–69°59′W) is close to the International Agua Negra Pass (Argentina – Chile). It is a typical mountainous postglacial landscape, with open valleys and elevations ranging from 4000 to 5774 m asl. Even though current glacial activity is limited, in the past it was an active relief modeling agent in the region. It is possible to observe erosive landforms such as cirques, glacial valleys arêtes and hanging valleys. Some accumulation landforms of glacial origin are longitudinal, basal and transversal moraines. The most representative periglacial landforms are detrital slopes, patterned grounds, rock glaciers, solifluction forms, talus cones and asymmetrical valleys, with south facing slopes being steeper than the north facing slopes.

2.1. Climate

Climate and topography varies along the length of the Andes Mountains. For this reason, the Cordillera de los Andes is divided into the Dry Andes, covering the region from 30° SL to 35°S, and the Wet Andes, covering the region south of 35° S. The Dry Andes section has been further divided into the Desert Andes from 30° to 31° S and the Central Andes from 31° to 35° S. In the Desert Andes, arid conditions limit the ice-and-snow formation to small patches on the highest peaks (Lliboutry et al., 1958). Here, most of the small ice-and-snow areas are found on the main range, which is the border between Argentina and Chile and precipitations occur during local storms.

Dry climates with rigorous winters, such as the one characterizing the Andes from 28° to 32°S latitudes, present very low temperatures in winter, short-lived summers, scarce precipitations and violent winds. The Dry Andes high-mountain region has its own local conditions, which differ from those of the larger climate zone to which it belongs. Because of the temperature drop at high altitudes, it is typically dry and cold. A negative thermal gradient of 0.5–1 C° with every 100 m of increase in altitude would result in higher relative humidity of the air and the occurrence of high precipitation on the windward slope and lower precipitation on the leeward side (rain shadow). Slope orientation, prevailing wind direction, and sunshine angle are also critical factors. The specific wind pattern and higher insolation in certain directions produces a differentiated topoclimate (topographical climate). Temperature is above freezing only during 4 months. From 3500 to 4000 m asl, temperatures range between −18 °C and 10 °C. Above 4300 m asl, the climate is characterized by perpetual ice, where the average temperature in the warmest month is below 0 °C. Between 4000 and 6000 m asl, precipitation occurs mainly as snow and hail. Below 4000 m, rain is scarce and very irregular; snow precipitation in the Cordilleran zone, north of San Juan is small and decreases considerably from south to north. Minetti et al. (1986) used annual averages from the meteorological stations in the surrounding areas and determined a regional precipitation average of 150 mm per year.

2.2. Geological and tectonic setting

The study area includes the Andean Frontal Cordillera, a geological province that is characterized by several elongated

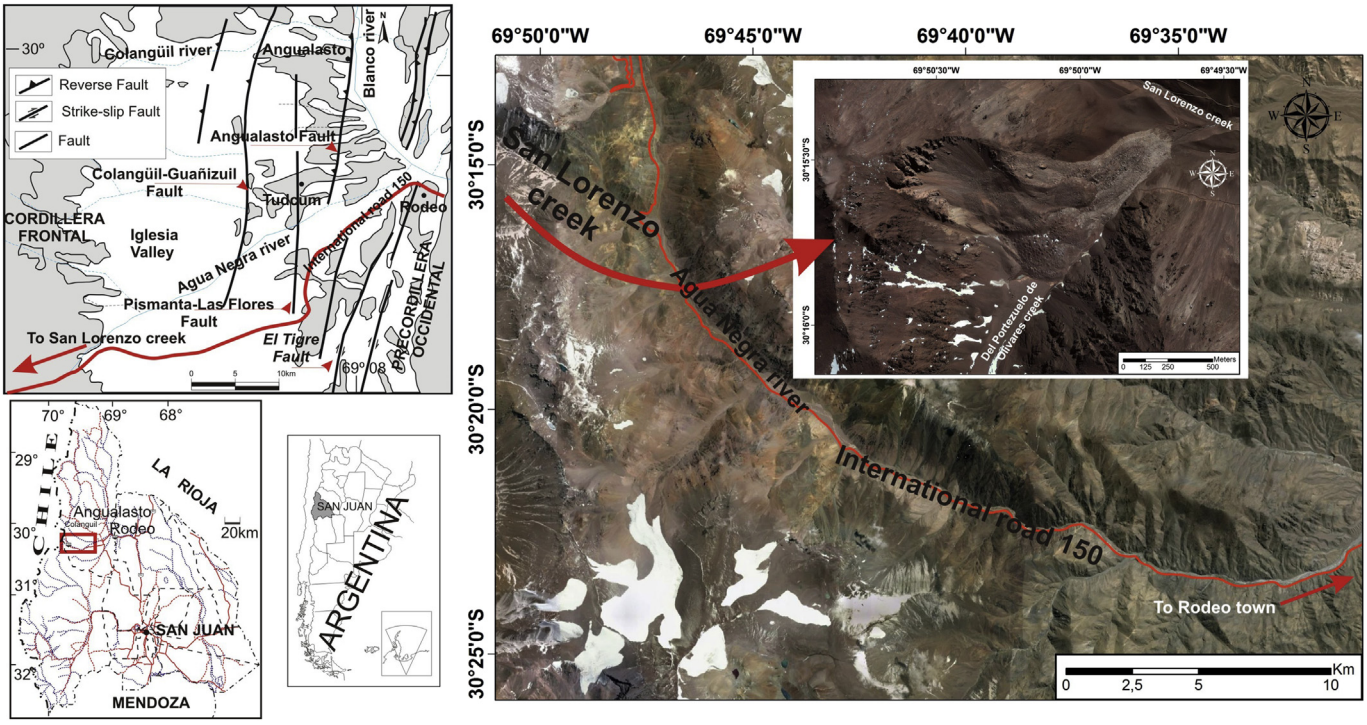

Fig. 1. San Juan Province, location of study area and the debris-rockslide. Main neotectonic structures modified from Perucca and Martos (2012).

mountainous ranges with a regional north–south trend. Their predominant formations are a series of Upper Paleozoic rocks which unconformably overlie a Middle Proterozoic substratum (Ramos, 1999) and highly deformed Lower Paleozoic sedimentary rocks. The oldest stratigraphic unit in the area is a Permian–Lower Triassic mesosilicic and silicic volcanic and igneous complex including pyroclastic, subvolcanic and intrusive rocks, the latter consisting of a lower andesite to dacite section and an upper rhyolitic section. The sequence continues with dacitic, rhyolitic and tuffs of upper Oligocene–Lower Miocene age resting unconformable on the Permo-Lower Triassic volcanic complex. Over these lie middle Miocene andesitic to dacitic volcanic rocks. The modern deposits, gravels, sands, and clay, occupy the valleys and river beds.

Between 28° and 32°S, the Nazca Plate subducts horizontally beneath the South American Plate, at about 100 km depth at a rate of 6.3 cm/year (Pardo Casas and Molnar, 1987; Somoza, 1998; Kendrick et al., 2003). This subhorizontalization started between 8 and 10 Ma, in close association with subduction of the ancient Juan Fernández Ridge (Jordan and Gardeweg, 1987; Ramos, 1988; Kay et al., 1991; Yáñez et al., 2001; Ramos et al., 2002; among others).

Evidence of tectonic activity during the Quaternary is found in the piedmonts of both Cordillera Frontal (Colangüil, Pismanta and Angualasto faults) and Precordillera (Fig. 1). The El Tigre fault (Bastías et al., 1984; Bastías, 1985; Siame et al., 1996, 1997; Fazzito et al., 2009) is located in the western piedmont of Precordillera. On the eastern piedmont of Cordillera Frontal, sub parallel faults, whose lengths reach several kilometers, affect Pleistocene alluvial fan levels. Main fault segments with activity during the Pleistocene, are distributed along the middle and distal portion of the Cordillera Frontal piedmont, such as Colangüil–Guañizuil, Pismanta-Las Flores-Bella Vista and Angualasto reverse faults, all of them trending N–S and located less than 50 km to the east of the slide. There are minor faults trending northwest to southeast and northeast to southwest (Perucca and Martos, 2012).

3. Methods

Fieldwork, high resolution satellite imageries (SPOT 5 with a 2.5 m spatial resolution, taken in 2007 and IKONOS with a 4 m spatial resolution, taken in 2006–2010–2011–2013) from Google Earth™, Landsat imageries (5 taken in 1990 and 7-TM taken in

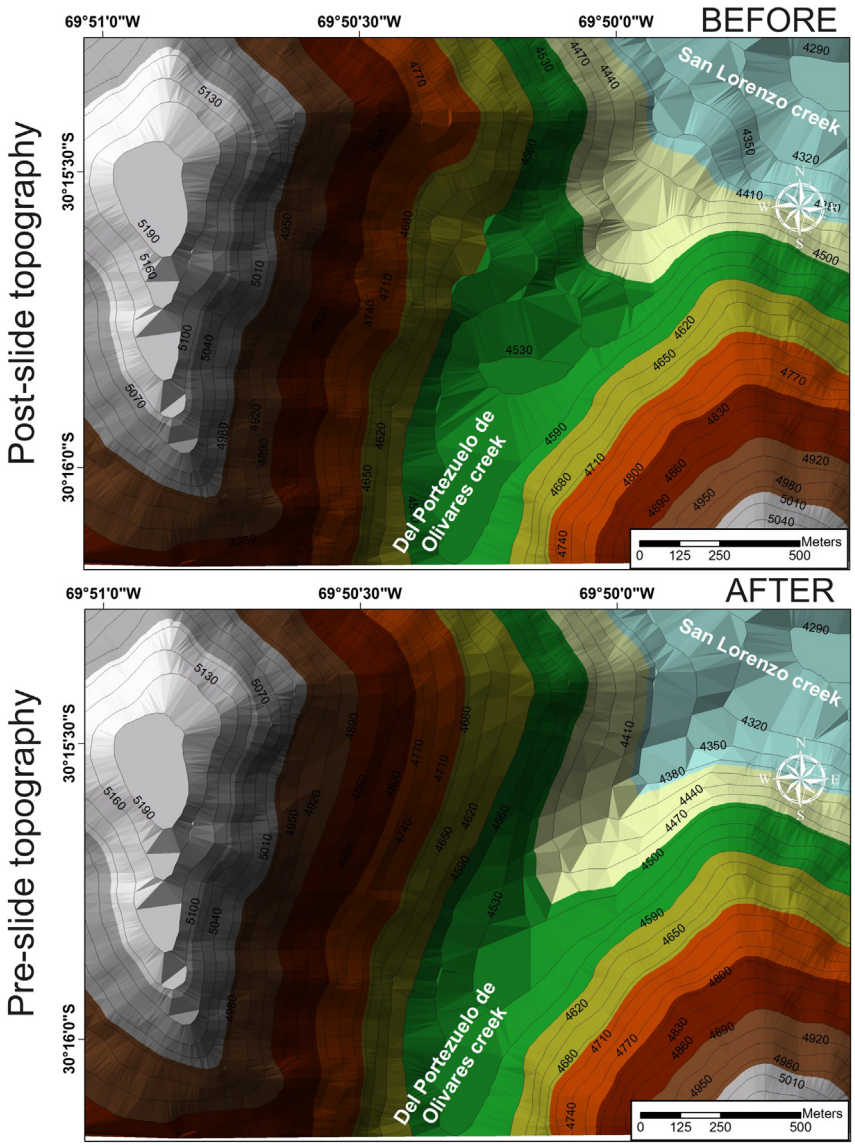

Fig. 2. DEMs showing the pre and post-slide topography.

2000) and ortho-rectified air photography mosaics (at 1:50,000 scale taken in 1980) were used to assess the characteristics of the rock-slide. The satellite imagery was georeferenced to a Geographical coordinate system (WGS84). The geological data were acquired from geologic maps published by the Servicio Geológico Minero Argentino (Argentine Mining Geologic Service) at a 1:100,000 scale.

The rock-slide total area (At), area of the displaced material (A_d), slope (S), perimeter length of the displaced material (P), the maximum (H, at the crown) and minimum heights (h, at the tip) and the slide relief (H_r) were first obtained and stored in vector format through manual digitization using GIS software. The morphometric parameters total length (L), length of the displaced mass (L_d), width of the displaced material (W_d), and width of the rupture zone (W_r) were measured according to the definitions to WP/WLI Suggested Nomenclature for Landslides (modified of IAEG, 1990). The length of the rupture zone (L_r) measurements present difficulties and are less accurate because of the toe of the surface of rupture is not exposed. For this reason L_r was directly estimated from satellite imagery interpretation by taking into account the original slopes around the slides.

Post-slide digital elevation model (DEM) representing the present topography was obtained from ASTER GDEM V2 (NASA, 2011). Pre-slide DEM was obtained by reshaping post-slide DEM by deleting points corresponding to slide debris and interpolating the pre-slide topography based on geomorphic observations (Fig. 2). Volume calculation of the slide involved measurement of the difference between pre and post-slide DEMs (Süzen and Doyuran, 2004). Cross sections (Fig. 3) obtained from the pre-slide and post-slide topography allowed for the estimation of the

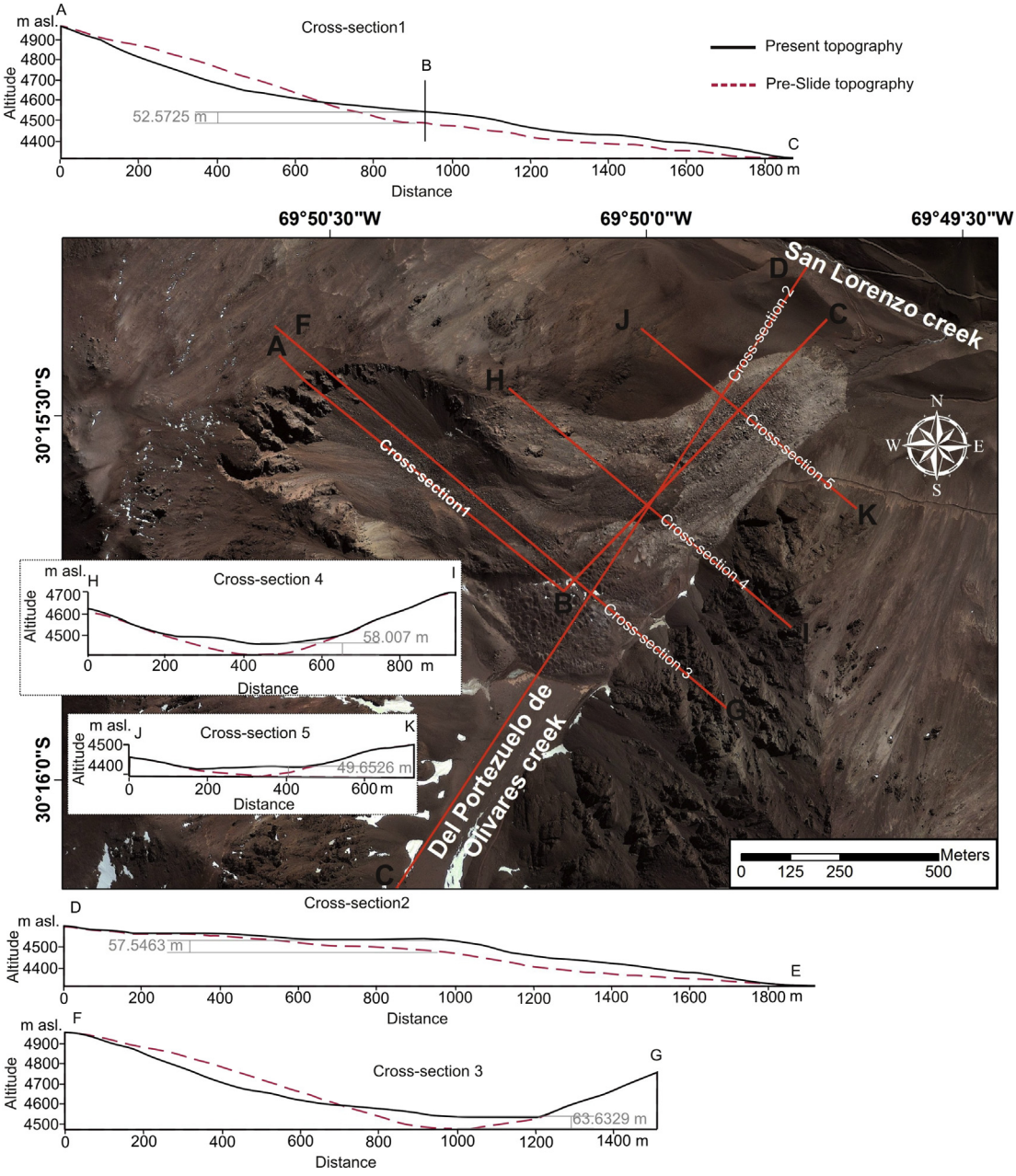

Fig. 3. Cross sections obtain from the pre-slide and post-slide topography and estimation of thickness.

depth of the rupture surface (D_r) and the depth of the displaced mass (D_d).

4. Results and discussion

On the portion of the Cordillera de Olivares under study, the landforms originated from the present glacial environment and prevail only at higher altitudes. Even though current glacial activity is limited, in the past it was an active agent in modeling the region's relief. Periglacial landforms have modified a Pleistocene glacial landscape which in the past occupied lower altitudes. The rocky layers adjacent to the glacier basins may have undergone reduction of buttressing and became gravitationally unstable. Here, lithological characteristics, absence of vegetation, pronounced slopes and climate settings have all favored landslides.

The studied debris-rockslide, previously identified by Elissondo (2007), is located on the Del Portezuelo de Olivares creek in The Cordillera de Olivares. The mode of failure was determined to be collapse sliding (Hungr and Evans, 2004). The basic bedrock geology of this part of the Frontal Andean was mapped as mesosilicic and silicic volcanic and igneous complex including pyroclastic, subvolcanic and intrusive rocks, which consist of a lower andesite to dacite section and an upper rhyolitic section. In these areas, Schrott (1996) established that currently the discontinuous permafrost is detected at 4150 m asl. This estimation, suggests that the failure zone was frozen at the time of the failure. The persistence of permafrost in the rock mass could explain the failure. The first effect of permafrost on rocks is to stabilize slopes by increasing mechanical properties (Krivonogova, 2009). With significant variations of temperature over the Holocene (Espizua, 1998, 1999; Coronato and Rabassa, 2007; Kilian and Lamy, 2012) permafrost thickness has varied with time, disappearing in low-elevation slopes. Therefore, an accelerated rise of the permafrost limit can be expected as a consequence of the present temperature increases. With permafrost boundary variations in rock slopes over long time periods, ice segregation may have acted as a contributory factor producing rock mass fractures, preferentially parallel to the slope, to a depth of a few tens of meters or more (Matsuoka et al., 1998).

Moreover, exceptionally heavier and warmer than usual precipitation might have occurred at higher latitudes as rain, making the snow line climb to more than 4000 m asl, and thus adding unusual amounts of water available to surface and subsurface runoff (Von Poschinger, 2002). This event would have brought exceptional load conditions to the slopes which would have impacted the generally small instability threshold. A rise in temperature would have significantly influenced the slope stability in glaciated and permafrost areas (Haeberli, 1992).

The main escarpment of the rockslide occurs along the SSW direction for about (W_r) 361.09 m. It consists of highly fractured rock with an average slope angle of 35° and is dissected by numerous rock chutes. The crown summit and tip are at altitudes 5023 and 4325 m asl respectively, giving a height difference (H_r) of 698 m. The slide deposits, involving 14.89 M m^3 of volcanic breccias of rhyolites, andesites, dacites and trachytes with angular to subrounded clasts (with a maximum diameter of 40 cm) cover an area of (A_d) 0.42 km^2. The cross-sections in Fig. 3 show that the accumulated material is generally between 49 and 63 m thick.

It is appropriate to take into account that the newly created "restored" surface was estimated from DEM of low resolution (30 m in our case), which subsequently limits the accuracy of the estimated rock slide volume and thickness. Fig. 2 shows the DEMs showing pre and post failure topography. A similar method of topographical reconstruction, using the intersection lines of interpolated structural features, has been presented by Süzen and Doyuran (2004); Oppikofer (2009); Esper Angillieri and Perucca (2013) and Esper Angillieri et al. (2014).

A Dr/Lr ratio value of 0.08 is characteristic of a rock slide (Skempton and Hutchinson, 1969). More details about geometry of the slide are presented in Table 1. The morphology in the run out area is very rough; the deposit has a gently convex-upward, lobate profile and a steep frontal ridge. The emplacement of the deposit mass dammed the valley from side to side; however drainage conditions are good because most of it is internal. Springs can be found at the toe of the slide (Figs. 1 and 3).

Table 1
Morphological parameters of the rock slide.

Parameters		Value
Altitude (H)	(Hmáx)	5023 m asl
	(Hmin)	4315 m asl
Slope angle (S)		26.43°
Slope aspect (S_a)		ESE
Total Length (L)		1788.79 m
Displaced material Length (Ld)		1349.09 m
Length of the rupture surface (Lr)		655.59 m
Depth of displaced material depth (Dd)		56.28 m
Depth of the rupture surface (D_r)		52.53 m
Width of the surface of rupture (Wr)		361.09 m
Width of the displaced material (Wd)		342.52 m
Total perimeter length (P)		4059.31 m
Area (A)	Total (At)	0.68 km^2
	Displaced material (Ad)	0.42 km^2
Estimated volume (V)		14.89 × 10^6 m^3

The evolution of the rock slide can be analyzed by means of a multi-temporal study with air photographs and satellite imagery for the period 1980–2013 (Fig. 4). Photographs taken in 1980 show the principal landslide deposit damming the Del Portezuelo de Olivares creek and flowing to the San Lorenzo creek. This slide was reactivated at least four more times with different movement that occurred sometime between 1980 and 2006.

Images from 1980, 1990, 2000, 2006, and 2013 enable the assessment of the rock slide dynamics showing the evolution of the remodeled body mobilized by rock slide processes. In photographs taken in 1980 the length between the main scarp and the slide deposit is 265.75 m. In LandSat imagery from 1990 to 2000 the main scarp cannot be adequately measured due to the low resolution of these images, but it is possible to distinguish geomorphic features related to slide #3. In the recent high-resolution images taken between 2006 and 2013 the rock-slide length increased to 504.97 m and it is possible to recognize two newer rock slide deposits pointing to successive events (Fig. 4).

The Cordillera Frontal and Iglesia valley have a low level of seismic activity. From 1929 to 2014 on average, only 6 magnitude 5 or greater earthquakes have been recorded in this large area. One large magnitude 6.5 earthquake (1938) has occurred in this region (Table 2). The three closest high magnitude earthquakes (Ms 6.5, 5.5 and 5.8) were located at distances of 30, 39 and 49 km respectively. The area has a low to moderate level of seismicity when compared to the more active seismic zones to the south, between 30° and 33° S. These intraplate earthquakes are not well understood, and the relationship between them and active faults is difficult to establish. Seismic activity is not considered to have been the ultimate triggering event. The mountainous front of Cordillera Frontal is sinuous. This, accompanied by glaciplanation processes, indicates periods of tectonic stability (Perucca and Martos, 2012).

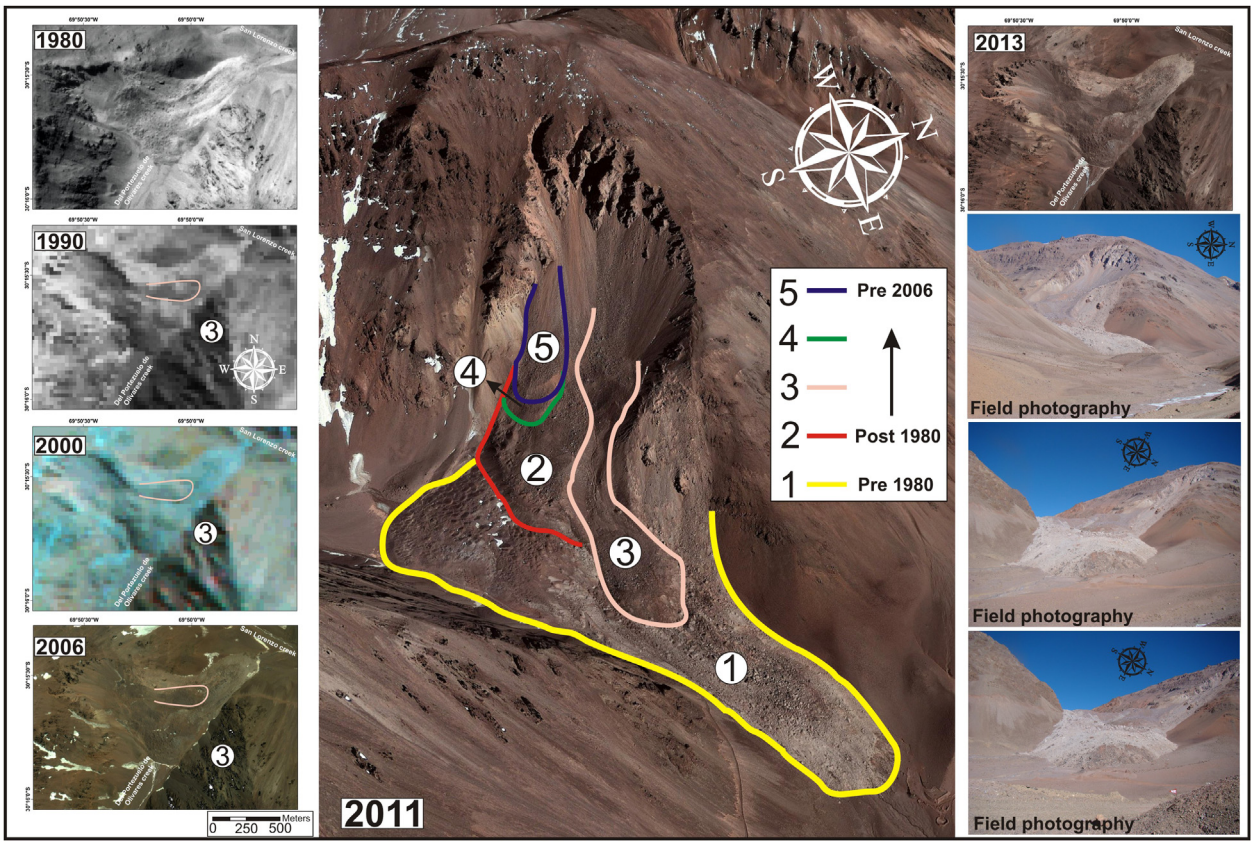

Fig. 4. Multitemporary evolution of the slide by comparing air photos (1980) and satellite images 1990, 2000, 2006, 2011 3D View (Google Earth™) and field photographs.

Table 2
Historical earthquakes from USGS-NEIC (2014).

Date	Time	Latitude	Longitude	Depth [km]	Magnitude
23/11/1929	12:32:00.00	−30.600	−69.700	0	5.4
23/06/1938	01:03:58.00	−30.500	−70.000	70	6.5
20/07/1969	10:00:14.70	−30.080	−69.730	122	4
28/11/1971	11:12:04.00	−29.909	−69.518	125	5.8
17/01/1973	19:25:49.50	−30.309	−69.401	57	4.5
14/12/1974	15:39:33.30	−30.284	−69.288	122	4.1
10/05/1978	23:06:00.80	−29.917	−68.858	33	5
06/05/1984	13:57:31.40	−30.549	−68.898	75.9	4.8
25/05/1984	18:05:26.39	−30.162	−69.378	121.4	4.7
18/08/1987	00:41:28.83	−30.575	−69.238	63.5	4.5
14/06/1990	23:04:33.14	−30.15	−69.409	117	4.9
31/07/1992	12:21:28.47	−30.329	−68.991	132.5	4.3
03/09/1995	13:21:42.91	−30.524	−68.899	124	4.3
06/10/1995	19:07:30.80	−30.049	−69.268	33	4.1
24/11/1995	04:28:58.04	−30.342	−69.176	72.4	4.1
29/08/1996	16:50:20.32	−30.373	−69.080	59.7	4.4
10/05/1999	08:47:25.04	−30.397	−69.163	65.2	5.2
30/11/2000	13:00:01.20	−30.004	−68.851	47.6	4
23/10/2001	21:41:15.90	−30.077	−68.919	3.1	4
10/11/2001	04:28:39.68	−30.306	−69.246	117.2	4.7
14/05/2002	16:18:52.70	−29.955	−70.028	126.1	4
31/07/2002	18:44:59.50	−30.518	−69.239	0	4
19/11/2002	04:14:20.10	−29.925	−69.036	128.4	4.8
09/04/2003	03:11:45.00	−30.273	−69.367	1.1	4.1
21/08/2003	19:14:40.78	−30.058	−69.983	112.5	4.5
15/12/2003	08:02:44.15	−30.386	−69.597	33	4
07/05/2004	22:08:14.10	−30.284	−69.368	55.9	4.2
30/11/2006	09:03:24.60	−30.292	−69.399	8.2	4.2
09/05/2007	05:35:49.00	−30.285	−69.435	1.4	4.1
24/02/2008	22:20:51.50	−30.475	−69.419	0.1	4.2

Table 2 (*continued*)

Date	Time	Latitude	Longitude	Depth [km]	Magnitude
02/03/2010	21:56:43.04	−30.257	−69.02	36.2	5.1
28/09/2010	17:41:52.00	−30.135	−69.601	116.7	4.4
03/05/2011	06:35:41.83	−30.232	−69.229	48.3	4.5
28/03/2013	14:28:04.00	−30.337	−69.332	45	4.7
24/05/2013	18:50:31.70	−30.51	−69.258	42.7	4.6
02/08/2013	15:33:03.00	−30.202	−69.526	15.8	4.3
08/02/2014	19:58:11.00	−30.129	−69.029	123	4.5

These results support the interpretation of a predominant role of climate on slope destabilization, although the effect of seismic activity cannot be ruled out completely. The effect of permafrost is, however, hard to know from direct field observations, and its importance in comparison with that of the other factors is still difficult to assess (Lebrouc et al., 2013).

5. Conclusions

Through field observation, aerial photography and high resolution satellite imagery interpretation and the use of tool such as Aster DEM, the main morphometric parameters of a large and active debris-rockslide have been measured. Although it was not possible to establish with certainty the triggering mechanisms of the debris-rockslide, the morphological features of the deposits and the analysis of seismic activity and weather conditions in the region

have provided sufficient tools for assuming that this could be associated with exceptional snow discharges and short and intense meltdowns. These elements, together with the inherent permafrost conditions, low resistance rocks and steep slopes, could have generated favorable conditions for triggering the slide. It is therefore important to stress the usefulness of using historical satellite images, seismic catalogs and weather charts data for the analysis of geomorphological events. Finally, the results presented in this paper could be included as another valuable tool for land use in planning, design and management of roads in periglacial areas.

Acknowledgements

The authors thank especially Peter T. Bobrowsky for his helpful comments. The authors acknowledge funding received from CONICET (Argentinean National Council of Scientific and Technological Research) and young researchers projects of CICITCA (Secretary of Science and Technology UNSJ) to support this research.

References

Ballantyne, C.K., 2002. Paraglacial geomorphology. Quaternary Science Reviews 21, 255–269.
Bastías, H., 1985. Fallamiento Cuaternario en la región sismotectónica de Precordillera. Tesis Doctoral de la Facultad de Ciencias Exactas, Físicas y Naturales. Universidad Nacional de San Juan, San Juan, Argentina, 160 pp.
Bastías, H., Weidmann, N., Pérez, M., 1984. Dos zonas de fallamiento Plio-Cuaternario en la Precordillera de San Juan. In: 9° Congreso Geológico Argentino 2, pp. 329–341.
Coronato, A., Rabassa, J., 2007. Late Quaternary in South America. In: Elias, S.A. (Ed.), Encyclopedia of Quaternary Science. Elsevier, Amsterdam, pp. 1101–1109.
Elissondo, M., 2007. Geomorfología de la quebrada del Agua Negra. Provincia de San Juan. In: Serie Contribuciones Técnicas. Peligrosidad Geológica N° 12. SEGEMAR – IGRM. Aires, 132 pp.
Esper Angillieri, M.Y., Perucca, L.P., 2013. Mass movement in Cordón de las Osamentas, de La Flecha river basin, San Juan, Argentina. Quaternary International 301, 150–157.
Esper Angillieri, M.Y., Perucca, L., Rothis, M., Tapia, C., Vargas, N., 2014. Morphometric characterization and Seismogenic sources relationships of a large scale rockslide. San Juan, Argentina. Quaternary International 352, 92–99.
Espizua, L.E., 1998. Quaternary glaciations in the Río Mendoza Valley, Argentine Andes. Quaternary Research 40, 150–162.
Espizua, L.E., 1999. Chronology of Late Pleistocene glacier advances in the Río Mendoza Valley, Argentina. Global and Planetary Change 22, 193–200.
Fazzito, S., Rapalini, A., Cortés, J., Terrizzano, C., 2009. Characterization of Quaternary faults by electric resistivity tomography in the Andean Precordillera of Western Argentina. Journal of South American Earth Sciences 28, 217–228.
Haeberli, W., 1992. Construction, environmental problems and natural hazards in periglacial mountain belts. Permafrost and Periglacial Processes 3 (2), 111–124.
Hungr, O., Evans, S.G., 2004. The occurrence and classification of massive rock slope failure. Felsbau 22, 16–23.
IAEG, 1990. Suggested nomenclature for landslides. Bulletin of the International Association of Engineering Geology 41, 13–16.
Jordan, T., Gardeweg, M., 1987. Tectonic evolution of the late Cenozoic Central Andes. In: Ben Avraham, Z. (Ed.), Mesozoic and Cenozoic Evolution of the Pacific Margins. Oxford University Press, pp. 193–207.
Kay, S., Mpodozis, C., Ramos, V., Munizaga, F., 1991. Magma source variations for mid-late Tertiary magmatic rocks associated with a shallowing subduction zone and a thickening crust in the central Andes (28° to 33° S). In: Harmon, R.S., Rapela, C.W. (Eds.), Andean Magmatism and its Tectonic Setting, Geological Society of America Special Paper 265, pp. 113–137.
Kendrick, E., Bevis, M., Smalley, R.J., Brooks, B., Vargas, R.B., Lauría, E., Fortes, L.P.S., 2003. The Nazca-South America Euler vector and its rate of change. Journal of South American Earth Sciences 16, 125–131.
Kilian, R., Lamy, F., 2012. A review of Glacial and Holocene paleoclimate records from southernmost Patagonia (49–55°S). Quaternary Science Reviews 53, 1–23.
Krivonogova, N.F., 2009. Characteristics of the composition, structure and physicomechanical properties of permafrost rock soil in massifs. Soil Mechanics and Foundation Engineering 46, 136–146.
Lebrouc, V., Schwartz, S., Baillet, L., Jongmans, D., Gamond, J.F., 2013. Modeling permafrost extension in a rock slope since the Last Glacial Maximum: application to the large Séchilienne landslide (French Alps). Geomorphology 198, 189–200.
Lliboutry, L., González, O., Simken, J., 1958. Les glaciers du désert Chilien. Association of International Hydrological Sciences 46, 291–300.
Matsuoka, N., Hirakawa, K., Watanabe, T., Haeberli, W., Keller, F., 1998. The role of diurnal, annual and millennial freeze-thaw cycles in controlling alpine slope stability. In: 7th International Conference on Permafrost. International Permafrost Association, Yellowknife, Canada, pp. 711–717.
Minetti, J.L., Barbieri, P.M., Carleto, M.C., Poblete, A.G., Sierra, E.M., 1986. El régimen de precipitación de la provincia de San Juan. Informe técnico 8. CIRSAJ-CONICET, San Juan.
NASA, 2011. ASTER Global Digital Elevation Map V2. http://gdem.ersdac.jspacesystems.or.jp.
Oppikofer, T., 2009. Detection, Analysis and Monitoring of Slope Movements by Highresolution Digital Elevation Models (Ph.D. thesis). Institute of Geomatics and Analysis of Risk, University of Lausanne, Lausanne, Switzerland.
Pardo Casas, F., Molnar, P., 1987. Relative motion of the Nazca (Farallón) and South America plate since Late Cretaceous times. Tectonics 6, 233–248.
Perucca, L., Martos, L., 2012. Geomorphology, tectonism and Quaternary landscape evolution of the central Andes of San Juan (30°S-69°W), Argentina. Quaternary International 253, 80–90.
Ramos, V.A., 1988. The tectonics of the central Andes, 30° to 33° S latitude. In: Clark, S., Burchfiel, D., Suppe, J. (Eds.), Processes in Continental Lithospheric Deformation, Geological Society of America, Special Paper, 218, pp. 31–54.
Ramos, V.A., 1999. Las provincias geológicas del territorio argentino. In: Caminos, R. (Ed.), Geología Argentina, Anales, vol. 29 (3). SEGEMAR, Buenos Aires, pp. 41–96.
Ramos, V.A., Cristallini, E.O., Pérez, D., 2002. The Pampean flat-slab of the Central Andes. Journal of South American Earth Sciences 15, 59–78.
Siame, L., Sebfuer, M., Bellier, O., Bourles, D., Castano, J., Araujo, M., Yiou, F., Raisbeck, G., 1996. Segmentation and horizontal slip-rate estimation of The El Tigre Fault Zone, San Juan Province (Argentina) from spot images analysis. In: 3° Symposium International sur la Géodynamique Andine, St. Malo (France), pp. 239–242.
Siame, L.L., Bourlès, D.L., Sébrier, M., Bellier, O., Castano, J.C., Araujo, M., Perez, M., Raisbeck, G.M., Yiou, F., 1997. Cosmogenic dating ranging from 20 to 700 ka of a series of alluvial fan surfaces affected by the El Tigre Fault, Argentina. Geology 25, 975–978.
Schrott, L., 1996. Some geomorphological–hydrological aspects of rock glaciers in the Andes (San Juan, Argentina). Zeitschrift fuer Geomorphologie SB104, 161–173.
Skempton, A.W., Hutchinson, J.N., 1969. Stability of natural slopes and Embankment foundations. In: Proceedings of the 7th International Conference on Soil Mechanics and Foundation Engineering. Sociedad Mexicana de Suelos, Mexico City, State of the Art Volume, pp. 291–340.
Somoza, R., 1998. Updated Nazca (Farallón)-South America relative motions during the last 40 My: implications for mountain building in the central Andean region. Journal of South American Earth Sciences 11 (3), 211–215.
Süzen, M.L., Doyuran, V., 2004. Data driven bivariate landslide susceptibility assessment using geographical information systems: a method and application to Asarsuyu Catchment, Turkey. Engineering Geology 71, 303–321.
USGS/NEIC, 2014. National Earthquake Information Center, World Data Center a for Seismology. Global Earthquake Search. United States Geological Survey, National Earthquake Information Center. http://earthquake.usgs.gov/earthquakes/eqarchives/epic.
Varnes, D.J., 1978. Slope movement types and processes. In: Schuster, R.J., Krizek, R.J. (Eds.), Landslides, Analysis and Control, Transportation Research Board, Washington, DC, Spec. Report 176, pp. 11–33.
Von Poschinger, A., 2002. Large rockslides in the Alps: a commentary of the contribution of G. Abele (1937-1994) and a review of some recent developments. In: Evans, S., DeGraff, J. (Eds.), Catastrophic Landslides: Effects, Occurrence, and Mechanisms, pp. 237–255.
Yáñez, G., Ranero, C., Von Huene, R., Díaz, J., 2001. Magnetic anomaly interpretation across the southern central Andes (32°-34°S): the role of the Juan Fernández Ridge in the late Tertiary evolution of the margin. Journal of Geophysical Research 106 (B4), 6325–6345.